Published April 5, 2004

JCB Article

Cytoplasmic foci are sites of mRNA decay in human cells

Nicolas Cougot, Sylvie Babajko, and Bertrand Séraphin

Équipe labellisée La Ligue, Centre de Génétique Moléculaire, Centre National de la Recherche Scientifique, 91198 Gif sur Yvette, France

Understanding gene expression control requires defining the molecular and cellular basis of mRNA turnover. We have previously shown that the human decapping factors hDcp2 and hDcp1a are concentrated in specific cytoplasmic structures. Here, we show that hCcr4, hDcp1b, hLsm, and rck/p54 proteins related to 5′–3′ mRNA decay also localize to these structures, whereas DcpS, which is involved in cap nucleotide catabolism, is nuclear. Functional analysis using fluorescence resonance energy transfer revealed that hDcp1a and hDcp2 interact in vivo in these structures that were shown to differ from the previously described stress granules. Our data indicate that these new structures are dynamic, as they disappear when mRNA breakdown is abolished by treatment with inhibitors. Accumulation of poly(A)$^+$ RNA in these structures, after RNAi-mediated inactivation of the Xrn1 exonuclease, demonstrates that they represent active mRNA decay sites. The occurrence of 5′–3′ mRNA decay in specific subcellular locations in human cells suggests that the cytoplasm of eukaryotic cells may be more organized than previously anticipated.

Introduction

mRNA degradation plays a key role in the regulation of gene expression by counterbalancing the effects of transcription. Analyses, mostly performed in yeast, have revealed five different exonucleolytic pathways leading to the destruction of eukaryotic mRNA. In the 5′–3′ mRNA decay pathway, shortening of the poly(A) tail is followed by cleavage of the mRNA cap, exposing the mRNA body to the 5′–3′ exonuclease Xrn1 (Caponigro and Parker, 1996). The 5′–3′ pathway appears to be the major route for mRNA degradation in yeast cells, and it is regulated by controlling the rates of deadenylation and modulating cap cleavage efficiency (Caponigro and Parker, 1996). Likewise, the nonsense-mediated decay (NMD) pathway involves decapping followed by 5′–3′ digestion of the mRNA. However, during NMD, these steps are specifically induced by the recognition of a premature stop codon present in mRNAs (Czaplinski et al., 1999; Maquat and Carmichael, 2001). The three other known eukaryotic mRNA turnover pathways, 3′–5′ decay, nonstop decay (NSD), and 3′–5′ NMD, rely on the activity of the exosome, a multisubunit complex endowed with 3′–5′ exonuclease activity (Mitchell and Tollervey, 2000; Butler, 2002). 3′–5′ decay acts on a fraction of the mRNAs lacking a poly(A) tail, whereas NSD targets mRNAs missing a proper stop codon. Finally, although the majority of mRNAs containing a premature nonsense codon are degraded by the NMD, a minority appears to be degraded by the 3′–5′ NMD pathway (Lejeune et al., 2003; Mitchell and Tollervey, 2003; Takahashi et al., 2003). Thus, NMD, NSD, and 3′–5′ NMD allow the removal of aberrant mRNAs and unspliced pre-mRNAs in the cytoplasm that could be deleterious to the cell (He et al., 1993; Frischmeyer et al., 2002; van Hoof et al., 2002). In addition to these exonucleolytic processes, several groups have reported endonucleolytic inactivation of specific mRNAs such as human transferrin or IGF-II mRNAs (Binder et al., 1994; van Dijk et al., 2001). Given the number and complexity of the pathways implicated in mRNA degradation, their relative contribution to global mRNA degradation in human cells remains to be established.

In eukaryotes, the majority of the mRNA degradation process is thought to occur in the cytoplasm after translation of the corresponding RNA molecules. However, degradation of mRNAs and pre-mRNAs also occurs to some extent in the nucleus. Thus, the 3′–5′ mRNA turnover pathway is implicated in the decay of pre-mRNAs in yeast nuclei (Bousquet-Antonelli et al., 2000). Similarly, the cellular location where the NMD process occurs has been the focus of numerous studies. Indeed, although NMD was shown to be cytoplasmic in yeast, it was found associated with the nucleus in metazoan cells (Ishigaki et al., 2001). However, this process also requires active translation to promote the

Address correspondence to B. Séraphin, Équipe labellisée La Ligue, Centre de Génétique Moléculaire, Centre National de la Recherche Scientifique, Avenue de la Terrasse, 91198 Gif sur Yvette, France. Tel.: 33 1 69 82 38 84. Fax: 33 1 69 82 38 77. email: seraphin@cgm.cnrs-gif.fr

Key words: cell cycle; FRET; green fluorescent protein; transcriptional and translational inhibitors; RNA stability

Abbreviations used in this paper: FRET, fluorescence resonance energy transfer; NMD, nonsense-mediated decay; NSD, nonstop decay.

The Journal of Cell Biology, Volume 165, Number 1, April 12, 2004 31–40
http://www.jcb.org/cgi/doi/10.1083/jcb.200309008

Published April 5, 2004

recognition of premature stop codon. Translation in metazoan cell nuclei has been reported (Iborra et al., 2001) but recent evidences suggested that this should be taken with caution (Bohnsack et al., 2002; Dahlberg et al., 2003; Nathanson et al., 2003). Therefore, it is currently believed that NMD occurs during a pioneering round of translation once the newly synthesized mRNAs reach the cytoplasm after export through the nuclear pore complex, thus, being closely associated with the nucleus (Ishigaki et al., 2001). Newly exported mRNA substrates for NMD are recognized through their association with the nuclear cap-binding complex that transits with them from the nucleus to the cytoplasm (Visa et al., 1996). They are also punctuated with exon junction complexes that mark the location of excised introns, thus, playing an important role in the recognition of premature stop codons (Le Hir et al., 2001). Another level of complexity in the degradation of mRNAs arises because the distribution of some mRNAs is not uniform in the cytoplasm (St Johnston, 1995). However, it is currently unknown how this parameter affects mRNA degradation. Thus, overall, the cellular organization of the mRNA degradation process remains to be analyzed.

Although several pathways for mRNA degradation have been observed and described in human cells (Couttet et al., 1997; Chen et al., 2001), the factors involved in these processes and their regulation have remained poorly characterized until recently. Several human factors implicated in mRNA decay have been identified based on their homology to yeast factors. This includes proteins involved in the 5′–3′ pathway, such as the hDcp2 and hDcp1a factors involved in cap cleavage (Lykke-Andersen, 2002; van Dijk et al., 2002; Wang et al., 2002), as well as proteins involved in the 3′–5′ pathway, such as subunits of the human exosome (Allmang et al., 1999; Raijmakers et al., 2003). Interestingly, characterization of these proteins revealed that they have activities similar to those of their yeast counterparts. While characterizing the human decapping enzyme, we demonstrated that the hDcp1a and hDcp2 proteins colocalize in new cytoplasmic structures (van Dijk et al., 2002). Lsm proteins and Xrn1, which are also involved in 5′–3′ mRNA decay and/or in NMD, were found also in these structures in human cells (Ingelfinger et al., 2002), while related structures where subsequently observed in yeast (Sheth and Parker, 2003). Human Dcp-containing bodies were subsequently identified to structures (GW bodies) containing the GW182 mRNA-binding protein of unknown function (Eystathioy et al., 2002, 2003). These intriguing observations led us to ask the following questions: (a) are other mRNA degradation factors localized in the same structures? (b) Are these structures identical or similar to previously described cytoplasmic granules? (c) Do these structures represent storage sites for mRNA decay factors or do they represent sites of active mRNA degradation? We have now addressed these issues, and the results of the experiments described in the following section indicate that these new dynamic structures present in the cytoplasm of human cells represent sites of active mRNA degradation.

Results

Additional factors linked to mRNA decay localize to cytoplasmic foci

We showed previously that hDcp1a and hDcp2, involved in the 5′–3′ mRNA decay pathway, colocalize in cytoplasmic foci (van Dijk et al., 2002). These structures, which are known as GW182- or Dcp-containing bodies, could represent storage sites for these factors or active sites of mRNA decay. In the latter case, we would anticipate that all factors involved in the same mRNA degradation pathway would also localize in these structures, whereas if they represent storage sites, only factors in excess would be expected to concentrate there. To discriminate between these possibilities, we decided to identify additional human factors with similarity to yeast proteins involved in mRNA decay and to determine their localization through the use of GFP reporter fusions. Because the Dcp proteins are known to be involved in the 5′–3′ mRNA decay pathway, we selected factors involved in this process. Thus, we used a cDNA encoding for a second human protein related to yeast Dcp1, which has been named hDcp1b (Lykke-Andersen, 2002; van Dijk et al., 2002). A group of seven proteins of the Sm family, Lsm1–7, has been shown to interact with the 5′–3′ exonuclease Xrn1 and to be required for mRNA decapping in yeast (Bouveret et al., 2000; Tharun et al., 2000). We selected hLsm3 and hLsm4, which belong to the cytoplasmic complex involved in 5′–3′ mRNA decay but also associate with the nuclear U6 snRNP as part of another Lsm protein complex (Bouveret et al., 2000), and hLsm1, which is specific for the cytoplasmic complex, for our work, as the corresponding cDNAs were already available (Salgado-Garrido et al., 1999). We also obtained a published cDNA encoding the human rck/p54 protooncogene (Lu and Yunis, 1992; Akao et al., 1995). This protein, containing a putative RNA helicase domain, is homologous to yeast Dhh1p that has been shown to interact with yDcp1 and to stimulate decapping in vitro (Coller et al., 2001; Fischer and Weis, 2002). rck/p54 has been proposed to play a role in translation initiation by restructuring some mRNAs (Akao et al., 2003), and Xp54, the *Xenopus laevis* homologue of rck/p54, was proposed to be a shuttling protein that associates with nascent mRNA in the nucleus and accompanies it to the cytoplasm to control translation (Minshall et al., 2001; Smillie and Sommerville, 2002). Decapping of the mRNA in the 5′–3′ pathway requires prior deadenylation of the mRNA substrate to generate an oligo(A)-containing species, therefore, we also included hCcr4 in our analysis. Indeed, hCcr4 is homologous to one of the two subunits of the yeast deadenylase and has been shown likewise to possess 3′ exonuclease activity in vitro (Chen et al., 2002). Finally, we also analyzed the localization of DcpS, a protein required for cap nucleotide breakdown after mRNA degradation in both the 5′–3′ and the 3′–5′ pathways (Wang and Kiledjian, 2001; Liu et al., 2002; van Dijk et al., 2003). Thus, DcpS served as a control for a general factor related to overall mRNA decay.

The coding sequences of these various factors were inserted downstream of a CMV promoter and the GFP coding sequence of a mammalian expression vector. Sequencing of

Published April 5, 2004

the resulting clones confirmed that the coding sequences were in-frame with the GFP coding sequence and ascertained the absence of unwanted mutations. These plasmids were introduced into HEK293 human embryonic kidney cells by transient transfection, and localization of the GFP-tagged proteins was assessed by microscopic observation of cells fixed 48 h after transfection and counterstaining with propidium iodide to reveal the location of nuclei. The GFP–hDcp1b fusion was found only in the cytoplasm, where it was nearly exclusively concentrated in bright foci (Fig. 1 A). hLsm1 was also mostly cytoplasmic. It was also enriched in foci even though a diffuse staining was also detected (Fig. 1 B). hLsm3 (and hLsm4; unpublished data) was more homogeneously distributed, which is consistent with its presence in two Lsm complexes, one being cytoplasmic and the second being nuclear. Nevertheless, a fraction was also enriched in cytoplasmic foci (Fig. 1 C). These results obtained for hLsm1, hLsm3, and hLsm4 are consistent with the localization data for endogenous or tagged hLsm proteins reported while this work was in progress (Ingelfinger et al., 2002; Eystathioy et al., 2003). rck/p54 also displayed a general diffuse staining with accumulation in a discrete number of cytoplasmic foci (Fig. 1 D). Interestingly, hCcr4 was exclusively cytoplasmic with several bright foci detectable over a more general diffuse staining (Fig. 1 E). The absence of hCcr4 from the nucleus is particularly surprising, as this factor was also proposed to play a role in transcription (Albert et al., 2000). Finally, the GFP–DcpS fusion was found to be nuclear (Fig. 1 F), whereas GFP alone was homogenously distributed in the cytoplasm of transfected cells in addition to some nuclear staining (not depicted). Specific staining was further demonstrated by the absence of cytoplasmic foci staining with GFP fused to Snu30 or some hDcp1a mutant (unpublished data). The latter results demonstrate that a cytoplasmic distribution with bright foci is not a general phenomenon but rather reflects the specific distribution induced by the passenger protein fused to GFP. We conclude from this analysis that the factors implicated in 5′–3′ degradation tested are all enriched in specific foci in the cytoplasm of human cells.

5′–3′ mRNA decay factors colocalize in hDcp1a-containing bodies

Our observations raised the possibility that all factors accumulating in cytoplasmic foci colocalize in a unique set of structures. To test this hypothesis, we transiently transfected HEK293 cells with GFP fusions and assayed simultaneously for the localization of endogenous hDcp1a by indirect immunofluorescence using a rabbit serum (van Dijk et al., 2002) and anti–rabbit IgG coupled to Cy5 as a secondary antibody. Thus, overlap of the Cy5 and GFP signals detected by confocal microscopy would reveal the presence of the factors in the same structures. The results demonstrate that hDcp1b (Fig. 2 A), hLsm1 (Fig. 2 B), hLsm3 (Fig. 2 C), rck/p54 (Fig. 2 D), and hCcr4 (Fig. 2 E) all colocalize with structures enriched in hDcp1a (Fig. 2, arrowheads). Overall, these results demonstrated that all the factors involved in 5′–3′ mRNA tested accumulate in a single type of cytoplasmic structure even though they show slightly different distribution patterns, with some giving in addition diffuse signals in the cytoplasm and/or the nucleus, whereas others were nearly exclusively present in these structures (Fig. 1 A, hDcp1b). These small differences may be attributed to different protein levels and/or to different kinetics of interaction of these proteins with hDcp1a-containing bodies. The specificity of these colocalization experiments is further demonstrated by the observation that factors not specif-

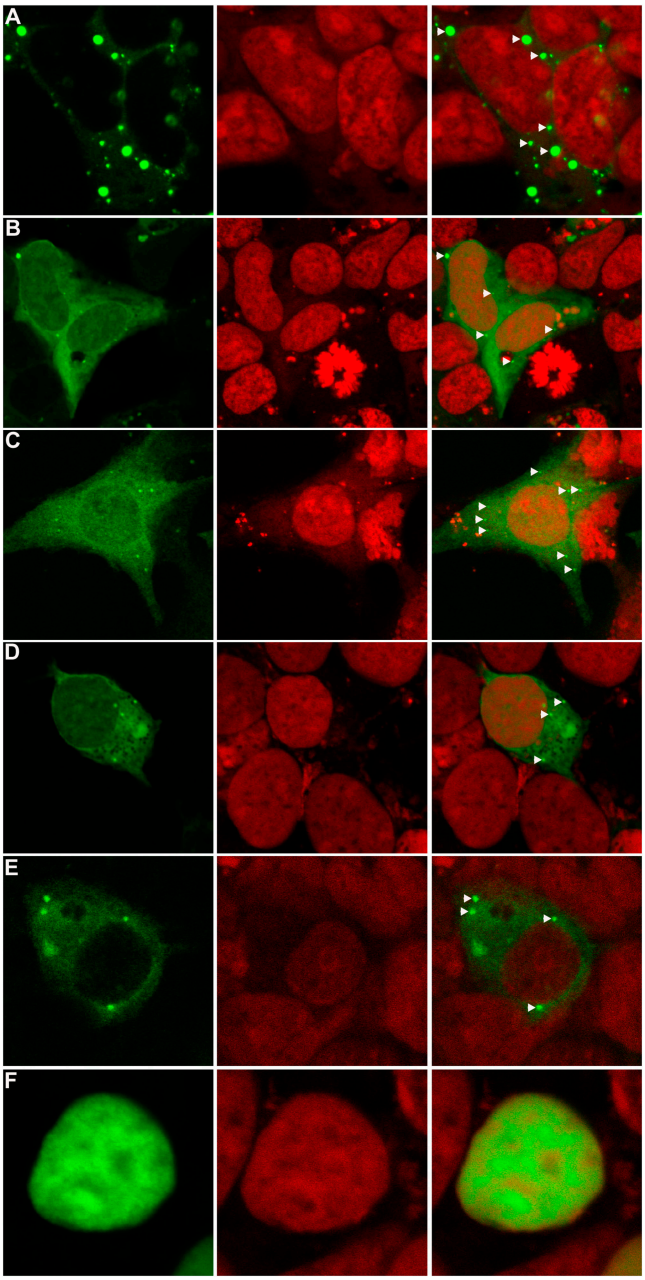

Figure 1. **Distribution of various mRNA decay factors in human cells.** Localization of GFP-hDcp1b (A), GFP-hLsm1 (B), GFP-hLsm3 (C), GFP-rck/p54 (D), GFP-hCcr4 (E), and GFP-DcpS (F). Left panels show GFP signal, middle panels show staining of the nucleus with propidium iodide, and right panels show overlays of the two signals. Different magnifications were used for the various panels to enhance visibility of important features. Some typical foci are indicated by arrowheads.

Published April 5, 2004

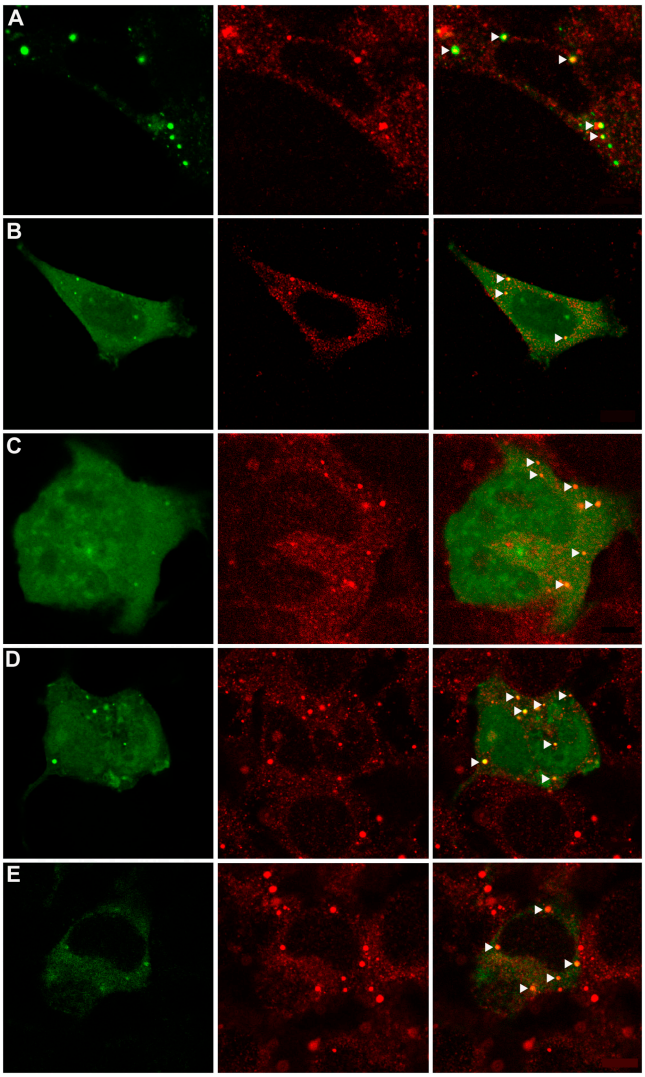

Figure 2. **Colocalization of mRNA decay factors with hDcp1a.** HEK293 cells were transiently transfected with GFP-hDcp1b (A), GFP-hLsm1 (B), GFP-hLsm3 (C), GFP- rck/p54 (D), or GFP-hCcr4 (E) and counterstained for hDcp1a. Left panels show GFP signals. Middle panels show immunostaining with rabbit anti-hDcp1a serum (1:1,000) and Fluorolink Cy5-labeled goat anti–rabbit IgG (1:1,000). Right panels show overlays of the two signals with arrowheads pointing to colocalizing proteins. Different magnifications were used for the various panels.

ically involved in the 5′–3′ pathway (Fig. 1 F, DcpS) or other cytoplasmic factors (see previous section) do not accumulate at the same location. Thus, these data are consistent with these foci representing sites of mRNA decay, although they do not formally exclude the "storage" hypothesis.

hDcp1a-containing bodies are not stress granules

Given the accumulation of factors involved in 5′–3′ mRNA decay in a unique structure, we asked whether or not these could correspond to previously described bodies. Survey of the bibliography shows that stress granules have a very similar distribution. Stress granules are cytoplasmic structures present in human cells that are related to RNA metabolism and that are induced upon oxidative stress (e.g., treatment

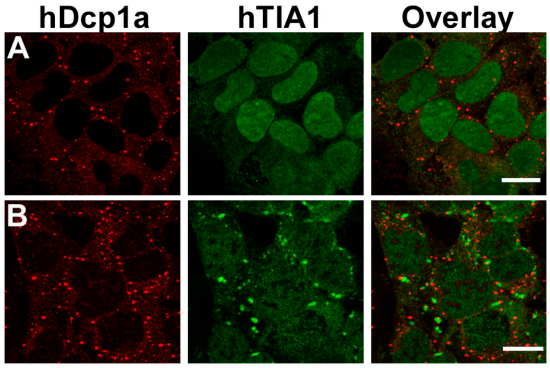

Figure 3. **hDcp1a-containing bodies are not stress granules.** Permeabilized HEK293 cells were incubated with rabbit anti-hDcp1a serum and anti–hTIA-1 mAbs (see Material and methods). (A) Untreated cells. (B) Cells treated with 0.5 mM sodium arsenite for 30 min. Left panels show the hDcp1a signal, middle panels show the hTIA-1 signal, and right panels show overlays of these two signals. Bars, 20 μm.

with arsenite; Kedersha and Anderson, 2002). To test if the structure containing mRNA decay factors could be stress granules, HEK293 cells were treated with 0.5 mM sodium arsenite and stained by indirect immunofluorescence with anti-hDcp1a rabbit serum and a known marker of stress granules, namely anti–TIA-1 monoclonal antibodies (Fig. 3). TIA-1 was mainly nuclear before treatment with sodium arsenite (Fig. 3 A, middle), which is consistent with its role in alternative splicing regulation (Förch et al., 2000), but accumulated in cytoplasmic stress granules after arsenite treatment as described previously (Fig. 3 B, middle; Kedersha et al., 2002). In contrast, sodium arsenite did not affect hDcp1a distribution (Fig. 3 B). Furthermore, an overlay of the hDcp1a and TIA-1 signals demonstrates that the great majority of these two proteins do not colocalize, even if both structures were closely localized in rare cases (Fig. 3 B). Thus, we conclude that hDcp1a-containing bodies are different from stress granules, at least under the conditions tested.

hDcp1a and hDcp2 interact in cytoplasmic foci

Analysis of yeast deletion mutants has demonstrated that mRNA decapping in vivo requires the simultaneous presence of the Dcp1 and Dcp2 proteins even though Dcp2 is catalytically active on its own in vitro (Beelman et al., 1996; Dunckley and Parker, 1999; van Dijk et al., 2002). Various analyses including two-hybrid tests, activity assays, and biochemical purifications have shown that Dcp1 and Dcp2 interact (Dunckley and Parker, 1999; Fromont-Racine et al., 2000; unpublished data). Similarly, hDcp1a and hDcp2 have been shown to coimmunoprecipitate (Lykke-Andersen, 2002). Based on the similarity between the yeast and the human proteins, we may assume that an interaction between hDcp1a and hDcp2 is required for their activity. Thus, we performed fluorescence resonance energy transfer (FRET) measurements to test whether or not these two proteins interact in vivo. For these experiments, we used previously described plasmids encoding hDcp1a or hDcp2 fused either to CFP or YFP proteins (van Dijk et al., 2002). The fluorescent pairs of CFP and YFP can serve as donor and acceptor, respectively, for FRET measurements with a calculated Förster distance (R0)

Published April 5, 2004

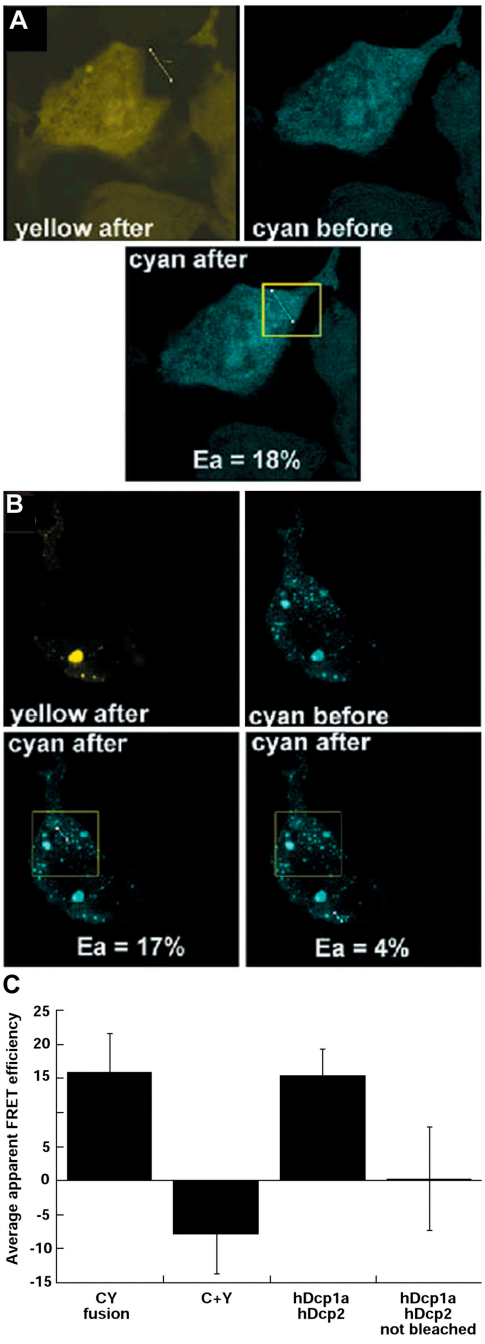

Figure 4. **hDcp1a and hDcp2 interact in cytoplasmic foci.** (A) Example of a FRET experiment where a fusion protein, CFP-YFP, was expressed in HEK293 cells as a positive control. A picture of the YFP signal was taken after photobleaching of a rectangular sector overlapping the cell (outlined in the CFP signal picture, bottom). A picture of the CFP signal was taken before (top right) and after (bottom) photobleaching of the YFP. Apparent FRET efficiency (18% for this experiment) was calculated as described in Materials and methods. (B) Example of a FRET experiment where CFP-hDcp1a and YFP-hDcp2 were expressed in HEK293 cells. Pictures were taken as described in A. Quantification of a foci in the bleached region shows an apparent FRET efficiency of 17% for this experiment (bottom left), whereas quantification of a foci out of the bleached region shows FRET efficiency of 4% (bottom right). (C) Histogram representing the average apparent FRET efficiency for the different constructions in different experiments. Error bars indicate the standard deviation from the independent measurements.

of 4.9 nm for unoriented molecules (Patterson et al., 2000). Owing to the presence of endogenous hDcp proteins in the cells and the variable expression of the fusion constructs, it is not possible to demonstrate FRET by using sensitized acceptor emission. However, FRET efficiency can be measured by acceptor photobleaching, which makes use of the quenching of the donor fluorescence when the excitation energy is transferred to the acceptor by FRET. After acceptor photobleaching, this quenching no longer occurs and the donor fluorescence increases. Quantification of this increase is a reliable measure of FRET (Miyawaki and Tsien, 2000; Wouters et al., 2001; Verveer et al., 2002).

We first established controls to measure FRET efficiencies. As positive control, HEK293 cells were transiently transfected with a plasmid encoding a CFP–YFP fusion. A clear FRET signal was detected (Fig. 4 A). The average apparent FRET efficiency over several experiments was 16% for this positive control (Fig. 4 C). In contrast, in HEK293 cells cotransfected with two independent vectors encoding CFP and YFP used as a negative control, the average apparent FRET efficiency was −8% (Fig. 4 C). Transiently transfected HEK293 cells expressing CFP-hDcp1a and YFP-hDcp2 demonstrated a clear FRET signal (Fig. 4 B, bottom left) with an average positive apparent FRET efficiency of 15% over several experiments (Fig. 4 C). Control quantification of foci out of the bleached region revealed no FRET signal (Fig. 4 B, bottom right) and the corresponding average apparent FRET efficiency was 0.3% (Fig. 4 C). These data indicate that hDcp1a and hDcp2 interact in vivo in cytoplasmic foci.

Translational inhibitors blocking mRNA decay induce a decrease in the number of cytoplasmic foci

If structures enriched in mRNA decay factors are actively involved in this process, we should expect them to disappear or to be reduced under a condition where mRNA decay is inhibited. In contrast, if they represent the site of mRNA decay factor storage, we should expect them to increase in number or size upon mRNA decay inhibition. Translational inhibitors such as cycloheximide are known to stabilize mRNAs (for review see Jacobson and Peltz, 1996; Ross, 1995) and represent a useful tool to discriminate between these two hypotheses. Thus, the effect of translation inhibitors on the distribution of cytoplasmic foci containing mRNA decay factors was assayed by microscopy to draw a link between mRNA degradation and presence of these structures. We treated HEK293 cells stably expressing a GFP–hDcp1a fusion with cycloheximide at 5 μg/ml, as this has been shown to result in complete inhibition of protein synthesis in mammalian cells (Pap and Cooper, 2002). Interestingly, addition of cycloheximide resulted in a near-complete disappearance of the cytoplasmic foci (Fig. 5, compare A with B). This effect was relatively rapid with an approximately fivefold reduction in the number of structures per cell already detectable 15 min after the addition of cycloheximide (Fig. 5 C). [^{35}S]methionine incorporation indicated that translation inhibition was essentially complete (>80%) and did not increase (variation +/−3%) after this time point (unpublished data). In contrast, addition of solvent alone did not affect the average number of hDcp1a-labeled foci per cell (Fig. 5 C). Western blot anal-

Published April 5, 2004

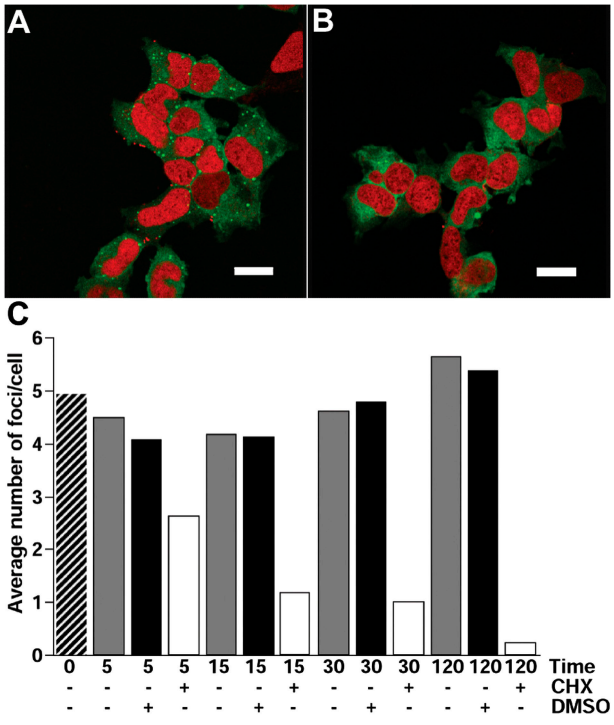

Figure 5. **hDcp1a-containing bodies disappear after treatment with cycloheximide.** HEK293 cells stably expressing hDcp1a were treated with 5 μg/ml cycloheximide for 5, 15, 30, and 120 min. Six fields randomly chosen were observed per time point, and number of foci per cell (covering ~170 cells) was counted and reported on a histogram. (A) Distribution of hDpc1a at time 0. (B) Distribution of hDcp1a after 2 h of treatment. Bars, 20 μm. (C) Histogram representing a time course evolution of the average number of foci. Black bars represent untreated cells, gray bars represent treatment with DMSO, white bars represent treatment with cycloheximide, and the shaded bar represents cells at time 0 before any treatment.

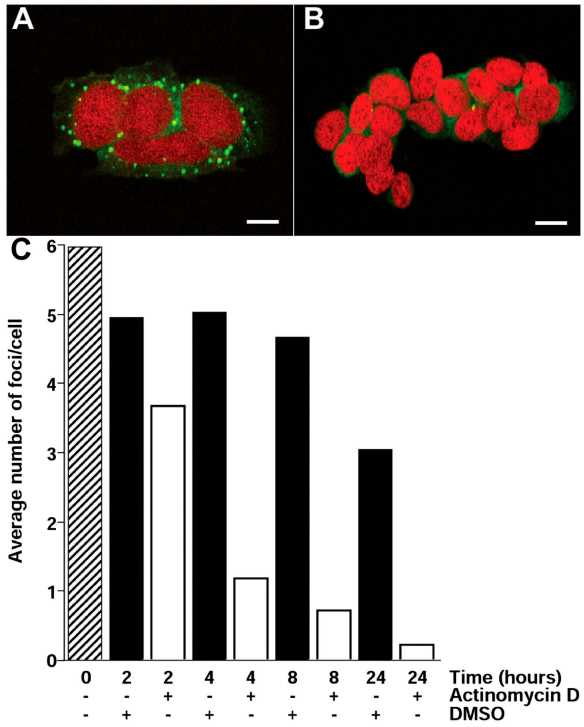

Figure 6. **hDcp1a-containing bodies disappear after treatment with actinomycin D.** HEK293 cells stably expressing hDcp1a were treated with 5 μg/ml actinomycin D for 2, 4, 8, and 24 h. Six fields randomly chosen were observed per time point and number of foci per cell was counted and reported on a graph. (A) Distribution of hDpc1a at time 0. (B) Distribution of hDcp1a after 24 h of treatment. Bars, 10 μm. (C) Histogram representing time course evolution of the average number of foci. Black bars represent treatment with DMSO, white bars represent treatment with actinomycin D, and the shaded bar represents cells at time 0 before any treatment.

ysis demonstrated that the decreased number of foci did not result from a decreased level of the GFP-tagged protein, as it was stable for several hours (unpublished data). Thus, these data demonstrate that cytoplasmic bodies disappear when translation and, consequently, mRNA decay are inhibited after treatment of the cells with cycloheximide. Similar results have been obtained with other translational inhibitors (unpublished data). Overall, these results provide a strong indication that the hDcp1a-containing bodies are actual sites of mRNA decay rather than storage sites for mRNA decay factors. This conclusion is further supported by the disappearance of these structures in mitosis, during which mRNA decay is also abolished (unpublished data). Furthermore, these data demonstrate the highly dynamic nature of the cytoplasmic structures containing 5′–3′ mRNA decay factors.

Ongoing transcription is required for body maintenance

If cytoplasmic foci are the actual sites of mRNA degradation, their presence should be dependent on the presence of substrate mRNAs. To test whether or not this is the case, we analyzed the number of hDcp1a-labeled foci in cells treated with the PolII inhibitor actinomycin D (5 μg/ml). Treatment of the cell line HEK293 stably expressing a GFP–hDcp1a fusion with actinomycin D lead to the near-complete disappearance of hDcp1a-containing bodies (Fig. 6, compare A with B). Quantitative analysis (Fig. 6 C) revealed that the actinomycin D effect was slower than that of cycloheximide, suggesting that it could be more indirect (e.g., requiring the near-complete disappearance of all mRNAs). Again, this effect was not detected in cells treated with solvent alone (Fig. 6 C), and it did not reflect the absence of the GFP–hDcp1a fusion because Western blot experiments demonstrated that the fusion protein was present at similar levels at all time points (not depicted). Thus, we conclude that ongoing transcription is required for maintenance of these cytoplasmic foci.

Poly(A)$^+$ RNA accumulates in hDcp2-containing structures after RNAi-mediated Xrn1 inactivation

If structures containing mRNA degradation factors are active mRNA decay centers, rather than storage sites, they should contain decay intermediates. However, such intermediates are difficult to detect due to their extremely short half-lives and low concentration. Because Xrn1 is the major 5′–3′ exonuclease responsible for degradation of mRNA bodies in the 5′–3′ and NMD pathways, we reasoned that its inactivation should lead to the accumulation of cognate intermediates. Thus, inactivating Xrn1 function using RNAi should result in the accumulation of RNA intermediates in hDcp2-contain-

Published April 5, 2004

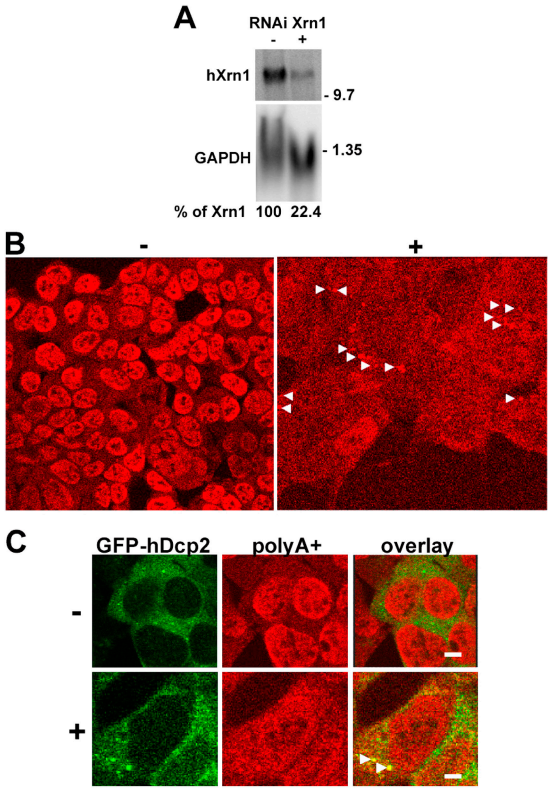

Figure 7. **poly(A)$^+$ RNA accumulate in hDcp2-containing bodies after RNAi-mediated Xrn1 inactivation.** (A) Northern blotting analysis of Xrn1 expression in control and Xrn1-inactivated cells. GAPDH mRNA was used as a loading control. Note that as the shRNA-expressing construct is stably integrated, reduced mRNA levels are expected to translate into corresponding reduced protein levels independently of the protein half-life except in the case of feed-back control. (B) poly(A)$^+$ RNA detection by FISH in control cells (left) and Xrn1-inactivated RNAi cells (right). Arrowheads indicate sites of accumulation of poly(A)$^+$ RNAs that may originate from incomplete deadenylation before decapping (Daugeron et al., 2001), overflow of the mRNA decay machinery resulting from Xrn1 inactivation, and/or degradation of NMD substrates. (C) Colocalization of GFP-hDcp2 and poly(A)$^+$ mRNA accumulation sites. Left panels show GFP signal of GFP-hDcp2 fusion, middle panels show Cy5 signal corresponding to poly(A)$^+$ RNAs, and right panels show overlay of the two signals, with arrowheads indicating colocalization. Bars, 4 μm.

ing structures, if they are involved in mRNA turnover. To test this possibility, we generated cells stably transfected with a plasmid governing the expression of shRNAs (Brummelkamp et al., 2002; Paddison et al., 2002) targeted against Xrn1 (or as control shRNAs with inactive sequence). These constructions were performed in cells stably expressing a GFP–hDcp2 fusion to allow the detection of the corresponding factor. In the resulting cells, shRNA expression induced a strong reduction of the Xrn1 mRNA level that dropped to 20% of its amount in control cells (Fig. 7 A). To detect mRNA decay intermediates, we reasoned that a fraction of the Xrn1 substrates should contain a poly(A) tail because decapping occurs when an oligo(A) tail is still present on mRNA 3′ ends and because NMD substrates can be degraded without complete deadenylation (Couttet and Grange, 2004). Thus, in Xrn1-depleted cells, poly(A)$^+$ RNAs were detected by FISH using a fluorescent Cy5-oligod(T)$_{20}$ probe (Buhler et al., 2002). Interestingly, a signal accumulated in discrete cytoplasmic foci (Fig. 7 B). No cytoplasmic accumulation of poly(A)$^+$ RNAs was observed in control cells (Fig. 7 B and not depicted), indicating that the poly(A)$^+$ signal present in the foci resulted from Xrn1 inactivation. Similar results were obtained with a second FISH protocol (Boehmer et al., 2003), confirming the validity of this observation (unpublished data). Colocalization experiments indicated that the site of poly(A)$^+$ RNA foci detected after RNAi-mediated Xrn1 inactivation corresponded to structures labeled with GFP-hDcp2 (Fig. 7 C). Together, these results indicate that cytoplasmic sites of mRNA decay factors accumulation represent active mRNA decay centers rather than storage structures.

Discussion

We previously identified hDcp2 as the catalytic subunit of the human decapping enzyme and observed, surprisingly, that it was enriched together with hDcp1a in cytoplasmic foci (van Dijk et al., 2002). In this paper, we asked if additional factors were present in these foci, if these foci were identical to some previously known cytoplasmic structures present in human cells, and if we could establish a link between these sites and the location of mRNA decay in human cells.

Our results demonstrate that all factors involved in 5′–3′ mRNA decay tested accumulate at least to some extent in a unique set of structures despite the fact that these proteins show a somewhat different overall distribution in cells. These proteins include factors involved in mRNA deadenylation (hCcr4), mRNA decapping (hDcp1a, hDcp1b, and hDcp2), as well as factors required for decapping activation (hLsm proteins and rck/p54). While this work was in progress, the colocalization of Lsm1–7 proteins with hDcp1a and/or hDcp2 in cytoplasmic foci was observed independently (Ingelfinger et al., 2002; Eystathioy et al., 2003). These foci also correspond to sites of accumulation of the 5′–3′ exonuclease Xrn1 (Bashkirov et al., 1997; Ingelfinger et al., 2002). This clustering of 5′–3′ mRNA decay factors contrasts with the nuclear location of DcpS (involved in cap nucleotide breakdown after mRNA decay in both the 3′–5′ and 5′–3′ mRNA decay) or with the location of the human exosome, which appears mostly concentrated in the nucleus and the nucleolus (Raijmakers et al., 2003). The accumulation of all factors tested in a single set of structures suggests that they represent the actual site of mRNA decay rather than storage sites. Indeed, in the latter case, one may have anticipated that some factors would be present in excess, and thus stored, whereas others, limiting for the degradation process, would not accumulate in the storage compartment. The recent observation that another RNA binding protein of unknown function, GW182, also localizes in the same structure in Hep-2 (Eystathioy et al., 2003) and HEK293 cells (unpublished data) also supports a role for these structure bodies in RNA metabolism. Further, we note that after the observation of the peculiar distribution of hDcp1a and hDcp2, a related observation was made in yeast cells (Sheth and Parker, 2003), even though in another study a more uniform distribution of the same proteins was reported (Tharun et al., 2000). The structures described in yeast contain the Dcp proteins, other mRNA decay factors, and mRNA decay intermediates (Sheth

Published April 5, 2004

and Parker, 2003). Given the similarity between the factors involved in mRNA decay in yeast and humans, this observation reinforces our conclusion that Dcp-containing bodies containing 5′–3′ mRNA decay factors are mRNA degradation centers. However, these structures are unlikely to be identical because hCcr4 is present in human bodies, whereas yeast Ccr4 is not detected in the yeast structures.

The use of translational inhibitors that are known to inhibit mRNA decay strongly suggests that cytoplasmic foci represent sites of mRNA decay. Indeed, translational inhibitors induced the disappearance rather than an enlargement of these structures. Our observation that two factors required for mRNA decapping interact in vivo in these foci also supports an active role for these structures. Further arguments for the functional nature of these bodies come from their absence from mitotic cells (unpublished data) or after transcriptional inhibition, consistent with the proposed absence of mRNA degradation under these conditions (Ross, 1997). To confirm this possibility, we inactivated Xrn1 by RNAi treatment to induce accumulation of otherwise undetectable mRNA decay intermediates. This strategy resulted in the accumulation of poly(A)$^+$ RNA in specific cytoplasmic foci that coincided with the location of the hDcp2 protein. These results indicate definitively that the cytoplasmic structures concentrating mRNA decay factors are active mRNA decay centers. Given that factors involved in decapping and 5′–3′ exonucleolytic trimming are also involved in NMD, it is tempting to speculate that this process occurs at the same location. Consistent with this possibility, hDcp1a and hDcp1b have been found to interact with hUpf1 that is involved in NMD (Lykke-Andersen, 2002). Even though our data indicate that 5′–3′ mRNA decay and NMD occur in a dedicated subcellular compartment, there is currently no obvious reason to explain why it should be so. One can hypothesize that this may serve to enhance the process through substrate channeling. Alternatively, a dedicated structure may prevent unwanted mRNA degradation in the cytoplasm. The cellular machinery involved in the targeting of the various components of these structures to their correct location and in the dynamic maintenance of these bodies remains to be identified. The localization of some individual factors gives also some interesting feedback information on their functions. Thus, rck/p54, the homologue of the yeast Dhh1 helicase, has been proposed to function in initiation of translation and translational control (Minshall et al., 2001; Smillie and Sommerville, 2002; Akao et al., 2003). In yeast, its homologue, Dhh1, interacts with Dcp1 and enhances decapping in vitro (Coller et al., 2001; Fischer and Weis, 2002). We observed that a fraction of rck/p54 localizes in cytoplasmic foci. Based on this result and on the homology of rck/p54 with yeast Dhh1, we propose that the protooncogene rck/p54 plays a role in activation of decapping as does the yeast homologue. The cytoplasmic location of hCcr4 is also informative, as this protein has been implicated in both transcription and mRNA degradation. The presence of an evolutionarily conserved nuclease domain (Chen et al., 2002), together with its accumulation in the cytoplasm and a (near-)complete nuclear exclusion (see Results), supports its role in mRNA degradation, even though a function in transcription cannot be ruled out. The exclusive nuclear localization of DcpS is also of interest. On the one hand, this feature appears evolutionarily conserved because the DcpS homologue from *Schizosaccharomyces pombe* also localizes in the nucleus (Salehi et al., 2002). On the other hand, we recently demonstrated that DcpS is involved in 7-methyl guanine–containing cap nucleotide breakdown in both the 5′–3′ and 3′–5′ pathways and hypothesized that this function might be required to prevent the deleterious consequences of incorporation of methylated G residues in RNA and/or DNA (van Dijk et al., 2003). The localization of DcpS in the nucleus, the main cellular site for transcription and DNA replication, is fully consistent with this possibility.

An interesting aspect of the cytoplasmic structures involved in mRNA decay is their dynamic nature. This feature will also probably be reflected in a heterogeneous composition and shape that will reflect the kinetic of association of individual factors with each structure. Thus, this may explain the slight differences in the number of foci and variation in staining intensities for individual factors. The observation of these new dynamic cytoplasmic structures raised the question of whether or not they corresponded to previously described bodies or to new cellular entities. Our data show clearly that they are not identical to stress granules even though both are highly dynamic and connected to mRNA metabolism. Other cytoplasmic structures related to RNA metabolism have been identified in specific cells, such as polar granules in *Caenorhabditis elegans* and *Drosophila melanogaster* oocytes and germ plasm in *X. laevis* oocytes (Micklem, 1995). However, given their restricted tissues distribution, such structures are unlikely to have a relation to the cytoplasmic mRNA degradation foci that we observe in human cells. Overall, these observations indicate that the cytoplasm may be more organized than previously anticipated. Interestingly, during the past years, results demonstrating that the eukaryotic nucleus is divided in highly dynamic but functionally distinct compartments have also accumulated (Lamond and Earnshaw, 1998). Further work will be necessary to understand the composition of the various cytoplasmic structures involved in mRNA metabolism and their functions in the precise control of gene expression.

Materials and methods

Plasmid constructions

cDNAs encoding hDcp1a or hDcp2 were cloned in peGFP-C2, peCFP-C1, and peYFP-C1 plasmids (CLONTECH Laboratories, Inc.; van Dijk et al., 2002). Plasmids harboring cDNAs corresponding to hCcr4 (a gift from L. Corbo, Centre Léon Bérard, Lyon, France; pBS2308), hDcp1b (pBS2326; IMAGE:5296928), hLsm1(pBS1457), hLsm3 (pBS981), hLsm4 (pBS1169), DcpS (pBS2419; IMAGE:1192708), and rck/p54 (from a rck/p54 expression plasmid; a gift from Y. Akao, Gifu International Institute of Biotechnology, Gifu, Japan) were used to construct GFP fusion in peGFP vectors (CLONTECH Laboratories, Inc.) using standard techniques (Sambrook et al., 1989). This procedure yielded the following constructs: GFP-hCCr4 (pBS2560), GFP-hDcp1b (pBS2408), GFP-hLsm1 (pBS2378), GFP-hLsm3 (pBS2343), GFP-hLsm4 (pBS2344), GFP-DcpS (pBS2563), and GFP-rck/p54 (pBS2564). The localization of these GFP fusions was consistent with the known localization of the cognate endogenous proteins except for hCcr4, p54/rck, hDcp1b, and DcpS that have not been tested in the absence of suitable antibodies. All constructs were verified by sequencing. YFP ORF was excised from peYFP-C1 and cloned in-frame at the COOH terminus of CFP in peCFP-C1 yielding the peCFP-YFP construct (pBS2559). The pBS2520 plasmid encoding shRNAs targeted against Xrn1 was generated by insertion of oligonucleotides generating the sequence C**GTCATGGCAAGGAGTTAC**CTTCAAGAGAGGTAACTCCTTGCCATGACTTTTTTGGAA (target sequence is in bold) between the BamHI and HindIII sites of pSilencer hygro™ (Ambion). As negative control, we used the shRNA encoding plasmid with no similarity to human genes (Ambion).

RNA isolation and Northern blotting analysis

Total RNA was extracted from 10^7 cells using Tri Reagent (Sigma-Aldrich) according the manufacturer's instructions. 50 μg of total RNA were electrophoresed onto 0.8% agarose/2 M formaldehyde gels and transferred to Hybond-N^+ nylon membranes (Amersham Biosciences). After prehybridization, blots were sequentially hybridized for 24 h at 50°C to 2×10^6 cpm/ml of hXrn1 and GAPDH cDNA probes (Multiprime DNA Labeling System; Amersham Biosciences). ImageQuant software was used for quantification.

Cell culture and transfection

Cell culture conditions were as described previously (van Dijk et al., 2002). For transient transfection, $\sim 3 \times 10^6$ HEK293 cells were transfected with 1 μg of plasmid DNA using the Effectene transfection reagent (QIAGEN). Stable transfections were performed using the same protocol. Cells were cultured for 2 d without selection agent and selected for 2–3 mo with 400 μg/ml G418 and/or 200 μg/ml hygromycin (Invitrogen). Cells were cloned and selected for expression of the fluorescent protein. Cells were treated with 5 μg/ml cycloheximide or actinomycin D dissolved in DMSO for the time indicated.

Indirect immunofluorescence and GFP localization

HEK293 cells were grown in DME Glutamax (Invitrogen) containing 10% FCS on clean glass slides to 70% confluence. The cells were washed with 1× PBS and fixed for 20 min in 4% PFA. After several washes, cells were permeabilized in 0.1% Triton X-100 for 10 min. Then, cells were saturated for 30 min with 0.2% BSA/1× PBS, and after several washes cells were immunostained for 1 h at 37°C with a rabbit anti-hDcp1a serum (1:1,000) or anti–hTIA-1 mAbs (provided by N. Kedersha, Harvard Medical School, Boston, MA; 1:1,000). After subsequent washes, cells were incubated 1 h at 37°C with secondary antibody, Fluorolink Cy5-labeled goat anti–rabbit IgG (Amersham Biosciences) for anti-hDcp1a serum or goat anti–mouse IgG FITC conjugated (Sigma-Aldrich) for anti–hTIA-1 antibodies (1:1,000). The anti-hDcp1a serum used for immunofluorescence revealed specifically hDcp1a in Western blotting analysis (van Dijk et al., 2002).

For localization of the GFP fusions, cells were fixed and treated as described in the previous paragraph and nuclei were stained for 30 min in a dark chamber with 5 μg/ml propidium iodide. For the colocalization experiments, HEK293 cells were transiently transfected either with GFP-hCcr4, GFP-hDcp1b, GFP-hLsm1, GFP-hLsm3, or GFP-rck/p54 as described in Cell culture and transfection. Then, cells were stained by immunofluorescence as described in the previous paragraph.

Preparations were analyzed using a confocal microscope (model RCS SP2; Leica) on an inverted stand using objectives HC Plan APO OS 100× oil NA 1.4. Specific excitation of GFP fusions was performed at 488 nm and collection of emitted light at 500–542 nm. Images were prepared using Leica software.

Acceptor photobleaching FRET

All data were obtained on a microscope (model RCS SP2; Leica). Samples were mounted as described in Indirect immunofluorescence and GFP localization, and images were acquired with objectives HC Plan APO OS 100× oil NA 1.4. Specific excitation of CFP-hDcp1a was performed at 458 nm and collection of emitted light at 495 nm. No emission from YFP-hDcp2 was observed in CFP channel. Images in the CFP channel were taken before and after photobleaching using the same sensitivity settings. YFP fusions were photobleached with full power excitation at 514 nm. Images of YFP-hDcp2 were taken after photobleaching and no CFP photobleaching was observed under these conditions. Apparent FRET efficiency was calculated using Leica software and according to the following equation: $Ea = (Ipost-Ipre)/Ipost$, where Ipost is the mean amplitude of CFP signal after YFP photobleaching, and Ipre is the mean amplitude of CFP signal before YFP photobleaching.

Fluorescent in situ hybridization

Poly$(A)^+$ RNAs were detected as described previously (Buhler et al., 2002). In brief, cells were grown on coverslips for 48 h, fixed with 4% PFA for 30 min, and permeabilized overnight at 4°C with 70% ethanol. Then, cells were rehydrated with 2× SSC/50% formamide and hybridization was carried out with 300 ng Cy5 oligod(T) in 15% formamide in a humidified dark chamber at 37°C for 3 h. After three washes with 2× SSC/50% formamide, coverslip were mounted and analyzed by confocal microscopy as described in Indirect immunofluorescence and GFP localization.

We thank Séraphin laboratory members for critical comments; Dr. N. Kedersha for antibodies; and Dr. Y. Akao and Dr. L. Corbo for the gift of plasmids. Microscopy was done in the core facility of the Centre National de la Recherche Scientifique (CNRS) campus supported by the Institut Fédératif de Recherche 87 (La plante et son environnement) and the Action de Soutien à la Technologie et la Recherche en Essonne program of the Conseil Général de l'Essonne with expert assistance from S. Brown and C. Talbot.

This work was funded by La Ligue pour la Recherche contre le Cancer (Equipe Labelisée), the Research Ministlry (grant ACI-BCMS), and the CNRS.

Submitted: 2 September 2003
Accepted: 5 March 2004

References

Akao, Y., O. Marukawa, H. Morikawa, K. Nakao, M. Kamei, T. Hachiya, and Y. Tsujimoto. 1995. The rck/p54 candidate proto-oncogene product is a 54-kilodalton D-E-A-D box protein differentially expressed in human and mouse tissues. *Cancer Res.* 55:3444–3449.

Akao, Y., H. Yoshida, K. Matsumoto, T. Matsui, K. Hogetu, N. Tanaka, and J. Usukura. 2003. A tumour-associated DEAD-box protein, rck/p54 exhibits RNA unwinding activity toward c-myc RNAs in vitro. *Genes Cells.* 8:671–676.

Albert, T.K., M. Lemaire, N.L. van Berkum, R. Gentz, M.A. Collart, and H.T. Timmers. 2000. Isolation and characterization of human orthologs of yeast CCR4-NOT complex subunits. *Nucleic Acids Res.* 28:809–817.

Allmang, C., E. Petfalski, A. Podtelejnikov, M. Mann, D. Tollervey, and P. Mitchell. 1999. The yeast exosome and human PM-Scl are related complexes of $3' \rightarrow 5'$ exonucleases. *Genes Dev.* 13:2148–2158.

Bashkirov, V.I., H. Scherthan, J.A. Solinger, J.M. Buerstedde, and W.D. Heyer. 1997. A mouse cytoplasmic exoribonuclease (mXRN1p) with preference for G4 tetraplex substrates. *J. Cell Biol.* 136:761–773.

Beelman, C.A., A. Stevens, G. Caponigro, T.E. LaGrandeur, L. Hatfield, D.M. Fortner, and R. Parker. 1996. An essential component of the decapping enzyme required for normal rates of mRNA turnover. *Nature.* 382:642–646.

Binder, R., J.A. Horowitz, J.P. Basilion, D.M. Koeller, R.D. Klausner, and J.B. Harford. 1994. Evidence that the pathway of transferrin receptor mRNA degradation involves an endonucleolytic cleavage within the 3′ UTR and does not involve poly(A) tail shortening. *EMBO J.* 13:1969–1980.

Boehmer, T., J. Enninga, S. Dales, G. Blobel, and H. Zhong. 2003. Depletion of a single nucleoporin, Nup107, prevents the assembly of a subset of nucleoporins into the nuclear pore complex. *Proc. Natl. Acad. Sci. USA.* 100:981–985.

Bohnsack, M.T., K. Regener, B. Schwappach, R. Saffrich, E. Paraskeva, E. Hartmann, and D. Görlich. 2002. Exp5 exports eEF1A via tRNA from nuclei and synergizes with other transport pathways to confine translation to the cytoplasm. *EMBO J.* 21:6205–6215.

Bousquet-Antonelli, C., C. Presutti, and D. Tollervey. 2000. Identification of a regulated pathway for nuclear pre-mRNA turnover. *Cell.* 102:765–775.

Bouveret, E., G. Rigaut, A. Shevchenko, M. Wilm, and B. Séraphin. 2000. A Sm-like protein complex that participates in mRNA degradation. *EMBO J.* 19: 1661–1671.

Brummelkamp, T.R., R. Bernards, and R. Agami. 2002. A system for stable expression of short interfering RNAs in mammalian cells. *Science.* 296:550–553.

Buhler, M., M.F. Wilkinson, and O. Muhlemann. 2002. Intranuclear degradation of nonsense codon-containing mRNA. *EMBO Rep.* 3:646–651.

Butler, J.S. 2002. The yin and yang of the exosome. *Trends Cell Biol.* 12:90–96.

Caponigro, G., and R. Parker. 1996. Mechanisms and control of mRNA turnover in *Saccharomyces cerevisiae*. *Microbiol. Rev.* 60:233–249.

Chen, C.Y., R. Gherzi, S.E. Ong, E.L. Chan, R. Raijmakers, G.J. Pruijn, G. Stoecklin, C. Moroni, M. Mann, and M. Karin. 2001. AU binding proteins recruit the exosome to degrade ARE-containing mRNAs. *Cell.* 107:451–464.

Chen, J., Y.C. Chiang, and C.L. Denis. 2002. CCR4, a 3′-5′ poly(A) RNA and ssDNA exonuclease, is the catalytic component of the cytoplasmic deadenylase. *EMBO J.* 21:1414–1426.

Coller, J.M., M. Tucker, U. Sheth, M.A. Valencia-Sanchez, and R. Parker. 2001. The DEAD box helicase, Dhh1p, functions in mRNA decapping and interacts with both the decapping and deadenylase complexes. *RNA.* 7:1717–1727.

Couttet, P., and T. Grange. 2004. Premature termination codons enhance mRNA decapping in human cells. *Nucleic Acids Res.* 32:488–494.

Couttet, P., M. Fromont-Racine, D. Steel, R. Pictet, and T. Grange. 1997. Messenger RNA deadenylylation precedes decapping in mammalian cells. *Proc. Natl. Acad. Sci. USA.* 94:5628–5633.

Czaplinski, K., M.J. Ruiz-Echevarria, C.I. Gonzalez, and S.W. Peltz. 1999. Should we kill the messenger? The role of the surveillance complex in translation termination and mRNA turnover. *Bioessays.* 21:685–696.

Published April 5, 2004

Dahlberg, J.E., E. Lund, and E.B. Goodwin. 2003. Nuclear translation: what is the evidence? *RNA.* 9:1–8.

Daugeron, M.C., F. Mauxion, and B. Séraphin. 2001. The yeast POP2 gene encodes a nuclease involved in mRNA deadenylation. *Nucleic Acids Res.* 29: 2448–2455.

Dunckley, T., and R. Parker. 1999. The DCP2 protein is required for mRNA decapping in *Saccharomyces cerevisiae* and contains a functional MutT motif. *EMBO J.* 18:5411–5422.

Eystathioy, T., E.K. Chan, S.A. Tenenbaum, J.D. Keene, K. Griffith, and M.J. Fritzler. 2002. A phosphorylated cytoplasmic autoantigen, GW182, associates with a unique population of human mRNAs within novel cytoplasmic speckles. *Mol. Biol. Cell.* 13:1338–1351.

Eystathioy, T., A. Jakymiw, E.K.L. Chan, B. Séraphin, N. Cougot, and M.J. Fritzler. 2003. The GW182 protein colocalizes with mRNA degradation associated proteins hDcp1and hLSm4 in cytoplasmic GW bodies. *RNA.* 9:1171–1173.

Fischer, N., and K. Weis. 2002. The DEAD box protein Dhh1 stimulates the decapping enzyme Dcp1. *EMBO J.* 21:2788–2797.

Förch, P., O. Puig, N. Kedersha, C. Martinez, S. Granneman, B. Séraphin, P. Anderson, and J. Valcárcel. 2000. The apoptosis-promoting factor TIA-1 is a regulator of alternative pre-mRNA splicing. *Mol. Cell.* 6:1089–1098.

Frischmeyer, P.A., A. van Hoof, K. O'Donnell, A.L. Guerrerio, R. Parker, and H.C. Dietz. 2002. An mRNA surveillance mechanism that eliminates transcripts lacking termination codons. *Science.* 295:2258–2261.

Fromont-Racine, M., A.E. Mayes, A. Brunet-Simon, J.C. Rain, A. Colley, I. Dix, L. Decourty, N. Joly, F. Ricard, J.D. Beggs, and P. Legrain. 2000. Genome-wide protein interaction screens reveal functional networks involving Sm-like proteins. *Yeast.* 17:95–110.

He, F., S.W. Peltz, J.L. Donahue, M. Rosbash, and A. Jacobson. 1993. Stabilization and ribosome association of unspliced pre-mRNAs in a yeast upf1- mutant. *Proc. Natl. Acad. Sci. USA.* 90:7034–7038.

Iborra, F.J., D.A. Jackson, and P.R. Cook. 2001. Coupled transcription and translation within nuclei of mammalian cells. *Science.* 293:1139–1142.

Ingelfinger, D., D.J. Arndt-Jovin, R. Luhrmann, and T. Achsel. 2002. The human LSm1-7 proteins colocalize with the mRNA-degrading enzymes Dcp1/2 and Xrnl in distinct cytoplasmic foci. *RNA.* 8:1489–1501.

Ishigaki, Y., X. Li, G. Serin, and L.E. Maquat. 2001. Evidence for a pioneer round of mRNA translation: mRNAs subject to nonsense-mediated decay in mammalian cells are bound by CBP80 and CBP20. *Cell.* 106:607–617.

Jacobson, A., and S.W. Peltz. 1996. Interrelationships of the pathways of mRNA decay and translation in eukaryotic cells. *Annu. Rev. Biochem.* 65:693–739.

Kedersha, N., and P. Anderson. 2002. Stress granules: sites of mRNA triage that regulate mRNA stability and translatability. *Biochem. Soc. Trans.* 30:963–969.

Kedersha, N., S. Chen, N. Gilks, W. Li, I.J. Miller, J. Stahl, and P. Anderson. 2002. Evidence that ternary complex (eIF2-GTP-tRNA(i)(Met))-deficient preinitiation complexes are core constituents of mammalian stress granules. *Mol. Biol. Cell.* 13:195–210.

Lamond, A.I., and W.C. Earnshaw. 1998. Structure and function in the nucleus. *Science.* 280:547–553.

Lejeune, F., X. Li, and L.E. Maquat. 2003. Nonsense-mediated mRNA decay in mammalian cells involves decapping, deadenylating, and exonucleolytic activities. *Mol. Cell.* 12:675–687.

Le Hir, H., D. Gatfield, E. Izaurralde, and M.J. Moore. 2001. The exon-exon junction complex provides a binding platform for factors involved in mRNA export and nonsense-mediated mRNA decay. *EMBO J.* 20:4987–4997.

Liu, H., N.D. Rodgers, X. Jiao, and M. Kiledjian. 2002. The scavenger mRNA decapping enzyme DcpS is a member of the HIT family of pyrophosphatases. *EMBO J.* 21:4699–4708.

Lu, D., and J.J. Yunis. 1992. Cloning, expression and localization of an RNA helicase gene from a human lymphoid cell line with chromosomal breakpoint 11q23.3. *Nucleic Acids Res.* 20:1967–1972.

Lykke-Andersen, J. 2002. Identification of a human decapping complex associated with hUpf proteins in nonsense-mediated decay. *Mol. Cell. Biol.* 22: 8114–8121.

Maquat, L.E., and G.G. Carmichael. 2001. Quality control of mRNA function. *Cell.* 104:173–176.

Micklem, D.R. 1995. mRNA localisation during development. *Dev. Biol.* 172: 377–395.

Minshall, N., G. Thom, and N. Standart. 2001. A conserved role of a DEAD box helicase in mRNA masking. *RNA.* 7:1728–1742.

Mitchell, P., and D. Tollervey. 2000. Musing on the structural organization of the exosome complex. *Nat. Struct. Biol.* 7:843–846.

Mitchell, P., and D. Tollervey. 2003. An NMD pathway in yeast involving accelerated deadenylation and exosome-mediated 3′→5′ degradation. *Mol. Cell.* 11:1405–1413.

Miyawaki, A., and R.Y. Tsien. 2000. Monitoring protein conformations and interactions by fluorescence resonance energy transfer between mutants of green fluorescent protein. *Methods Enzymol.* 327:472–500.

Nathanson, L., T. Xia, and M.P. Deutscher. 2003. Nuclear protein synthesis: a re-evaluation. *RNA.* 9:9–13.

Paddison, P.J., A.A. Caudy, E. Bernstein, G.J. Hannon, and D.S. Conklin. 2002. Short hairpin RNAs (shRNAs) induce sequence-specific silencing in mammalian cells. *Genes Dev.* 16:948–958.

Pap, M., and G.M. Cooper. 2002. Role of translation initiation factor 2B in control of cell survival by the phosphatidylinositol 3-kinase/Akt/glycogen synthase kinase 3beta signaling pathway. *Mol. Cell. Biol.* 22:578–586.

Patterson, G.H., D.W. Piston, and B.G. Barisas. 2000. Forster distances between green fluorescent protein pairs. *Anal. Biochem.* 284:438–440.

Raijmakers, R., W.V. Egberts, W.J. van Venrooij, and G.J. Pruijn. 2003. The association of the human PM/Scl-75 autoantigen with the exosome is dependent on a newly identified N terminus. *J. Biol. Chem.* 278:30698–30704.

Ross, J. 1995. mRNA stability in mammalian cells. *Microbiol. Rev.* 59:423–450.

Ross, J. 1997. A hypothesis to explain why translation inhibitors stabilize mRNAs in mammalian cells: mRNA stability and mitosis. *Bioessays.* 19:527–529.

Salehi, Z., L. Geffers, C. Vilela, R. Birkenhager, M. Ptushkina, K. Berthelot, M. Ferro, S. Gaskell, I. Hagan, B. Stapley, and J.E. McCarthy. 2002. A nuclear protein in *Schizosaccharomyces pombe* with homology to the human tumour suppressor Fhit has decapping activity. *Mol. Microbiol.* 46:49–62.

Salgado-Garrido, J., E. Bragado-Nilsson, S. Kandels-Lewis, and B. Séraphin. 1999. Sm and Sm-like proteins assemble in two related complexes of deep evolutionary origin. *EMBO J.* 18:3451–3462.

Sambrook, J., E.J. Fritsch, and T. Maniatis. 1989. Ligation of cohesive termini. *In* Molecular Cloning: A Laboratory Manual. Cold Spring Harbor Laboratory Press, Cold Spring Harbor, NY. 1.68–1.69.

Sheth, U., and R. Parker. 2003. Decapping and decay of messenger RNA occur in cytoplasmic processing bodies. *Science.* 300:805–808.

Smillie, D.A., and J. Sommerville. 2002. RNA helicase p54 (DDX6) is a shuttling protein involved in nuclear assembly of stored mRNP particles. *J. Cell Sci.* 115:395–407.

St Johnston, D. 1995. The intracellular localization of messenger RNAs. *Cell.* 81: 161–170.

Takahashi, S., Y. Araki, T. Sakuno, and T. Katada. 2003. Interaction between Ski7p and Upf1p is required for nonsense-mediated 3′-to-5′ mRNA decay in yeast. *EMBO J.* 22:3951–3959.

Tharun, S., W. He, A.E. Mayes, P. Lennertz, J.D. Beggs, and R. Parker. 2000. Yeast Sm-like proteins function in mRNA decapping and decay. *Nature.* 404:515–518.

van Dijk, E.L., J.S. Sussenbach, and P.E. Holthuizen. 2001. Kinetics and regulation of site-specific endonucleolytic cleavage of human IGF-II mRNAs. *Nucleic Acids Res.* 29:3477–3486.

van Dijk, E., N. Cougot, S. Meyer, S. Babajko, E. Wahle, and B. Séraphin. 2002. Human Dcp2: a catalytically active mRNA decapping enzyme located in specific cytoplasmic structures. *EMBO J.* 21:6915–6924.

van Dijk, E., H. Le Hir, and B. Séraphin. 2003. DcpS can act in the 5′-3′ mRNA decay pathway in addition to the 3′-5′ pathway. *Proc. Natl. Acad. Sci. USA.* 100:12081–12086.

van Hoof, A., P.A. Frischmeyer, H.C. Dietz, and R. Parker. 2002. Exosome-mediated recognition and degradation of mRNAs lacking a termination codon. *Science.* 295:2262–2264.

Verveer, P.J., A.G. Harpur, and P.I.H. Bastiaens. 2002. Imaging protein interactions by FRET microscopy. *In* Protein-Protein Interactions. E. Golemis, editor. Cold Spring Harbor Laboratory Press, Cold Spring Harbor, NY. 181–214.

Visa, N., E. Izaurralde, J. Ferreira, B. Daneholt, and I.W. Mattaj. 1996. A nuclear cap-binding complex binds Balbiani ring pre-mRNA cotranscriptionally and accompanies the ribonucleoprotein particle during nuclear export. *J. Cell Biol.* 133:5–14.

Wang, Z., and M. Kiledjian. 2001. Functional link between the mammalian exosome and mRNA decapping. *Cell.* 107:751–762.

Wang, Z., X. Jiao, A. Carr-Schmid, and M. Kiledjian. 2002. The hDcp2 protein is a mammalian mRNA decapping enzyme. *Proc. Natl. Acad. Sci. USA.* 99: 12663–12668.

Wouters, F.S., P.J. Verveer, and P.I. Bastiaens. 2001. Imaging biochemistry inside cells. *Trends Cell Biol.* 11:203–211.